Heat capacity of $YBa_2Cu_3O_{7-\delta}$ crystals along the H_{c2} line

S. E. Inderhees
Naval Research Laboratory, Washington, D.C. 20375

M. B. Salamon, J. P. Rice, and D. M. Ginsberg
Department of Physics and Materials Research Laboratory, University of Illinois, 1110 West Green Street, Urbana, Illinois 61801
(Received 12 July 1991; revised manuscript received 12 June 1992)

We report high-resolution ac heat-capacity measurements on $YBa_2Cu_3O_{7-\delta}$ crystals near the critical temperature, several of which display untwinned regions comprising at least 50% of the sample volume. A λ-like anomaly is observed, indicative of an exceptionally short $T=0$ Ginzburg-Landau coherence length in this material. If the fluctuations are assumed to be Gaussian corrections to mean-field behavior, the data are best described by three-dimensional fluctuations of a two-component order parameter, with the underlying BCS step indicating strong-coupling behavior. However, a more complicated order parameter or a logarithmic (critical) divergence cannot be ruled out on statistical grounds. Application of a magnetic field **B** broadens the transition and reduces the amplitude of the anomaly with little or no apparent shift in the onset of superconductivity; the effects are more pronounced for **B** parallel to the *c* axis than for **B** in the *ab* plane. These results are not consistent with mean-field theory, but may be understood in the context of critical finite-size scaling. This approach exploits the well-known dimensional reduction for superconductors in a magnetic field.

INTRODUCTION

It is by now well established that fluctuation effects play an important role near the critical temperature of $YBa_2Cu_3O_{7-\delta}$, most clearly manifested in a λ-like heat-capacity transition.[1-5] Estimates[6,7] of the critical region—where fluctuations dominate—use the Ginzburg criterion[8] to predict a width of order $T_g=0.1$ K above and below T_c. The crossover regime between classical and critical behavior may therefore lie in the experimentally accessible range. The Ginzburg criterion is based on the assumption that the crossover occurs when the leading correction to the mean-field (MF) heat capacity is on the order of the MF step itself. This first-order estimate can be expressed[8] in the form

$$T_g=2T_c\left[\frac{k_B/8\pi\xi_0^3}{\Delta C(T_c)}\right]^2, \tag{1}$$

where ξ_0 is the low-temperature Ginzburg-Landau coherence length and $\Delta C(T_c)$ is the MF specific-heat discontinuity at T_c. More recently, Fisher, Fisher and Huse[9] considered the effect of higher-order corrections and find these to become significant while the leading-order correction is still quite small relative to the MF jump. From this they conclude that the Ginzburg criterion actually underestimates T_g by a factor as large as 25. If so, T_g is actually of order 1 K, and true critical fluctuations may be observable within a few degrees of T_c.

Classic superconductors with short coherence lengths show a steplike transition that broadens slightly with increasing field, accompanied by the usual reduction of T_c.[10] However, application of a magnetic field has been shown to broaden and suppress the heat-capacity transition of $YBa_2Cu_3O_{7-\delta}$, with little or no change in the onset temperature.[11] The (MF) analyses of Thouless,[12] of Lee and Shenoy,[13] and others[14,15] are based on the observation that the applied field forces the superconducting electrons to move in Landau orbitals perpendicular to the field. As a result, the field decreases the effective dimensionality of the fluctuations from three to one, leading to behavior similar to the Ginzburg-Landau model in one dimension.[12] We will demonstrate that the $C(H,T)$ data for $YBa_2Cu_3O_{7-\delta}$ are inconsistent with these MF approaches.

According to the conventional picture, the phase transition of a superconductor is not preserved in an applied field; only in zero field does the coherence length diverge at T_c, limited only by sample size or inhomogeneities. In an applied field, $\xi(T_c(H))$ perpendicular to the applied field is limited by the lowest-order Landau radius $a_0\cong(\phi_0/2\pi H)^{1/2}$; it is electrons in this level that are the first to reach $T_c(H)$. Because the long-range order is destroyed, a superconductor in an applied field is similar[16] to other systems where the coherence length is constrained, for example, thin films of ^{4}He near T_λ,[17] to which the finite-size scaling[18] (FSS) formalism has been successfully applied.

In this paper, we present results of high-resolution heat-capacity measurements of $YBa_2Cu_3O_{7-\delta}$ near T_c in fields up to 7 T applied both parallel and perpendicular to the crystalline *c* axis. Least-squares analysis of the zero-field data shows that, if the fluctuations are assumed to be Gaussian, the data are best described in terms of three-dimensional fluctuations of a two-component order parameter. However, the zero-field data may also be fit satisfactorily with a logarithmic (critical) divergence. In a separate paper[19] we will describe a crossover procedure that combines the features of mean-field and critical behavior to fit the entire range of data, and confirms that

critical effects are important very close to T_c. However, we find that the in-field data cannot be explained in terms of MFT. Rather, we find that the data are better described in terms of critical finite-size scaling, and are consistent with a limiting length scale $L \propto H^{-1/2}$.

EXPERIMENT

Single-crystal samples were produced at the University of Illinois.[20] The ingredients are first ground into a uniform powder, placed in an yttria-stabilized zirconia crucible, and heated to 980 °C in air in a box furnace for several hours. During a very slow cooling to 830 °C, crystal growth takes place. The samples are then reannealed under flowing oxygen. The majority of crystals are twinned platelets of dimension roughly $1\times1\times0.05$ mm^3. This growth method also produces a small percentage of crystals with large untwinned regions which were used for the specific-heat measurements reported here. Table I lists the characteristics of the three samples used in this study. Sample YC104 displays a single-domain region accounting for approximately 80% of the sample's volume. For further screening of the samples, the magnetic susceptibility was measured as a function of temperature in a commercial SQUID-based susceptometer. Figure 1 shows a typical low-field scan. In the zero-field-cooled scan, the data approach $\chi=-1/4\pi$, indicating complete or near-complete flux expulsion.

In the ac calorimetry technique,[21] modulated light incident on the front face of the sample induces minute oscillations T_{ac} of the sample temperature, measured by a thermocouple junction attached to the back face. Within an appropriate range of frequencies T_{ac} is inversely proportional to the heat capacity of the sample. The contributing addenda are reduced to a minimum when light pulses, rather than a heater attached directly to the sample, are used.

A schematic of the ac calorimeter is shown in Fig. 2. The sample is attached with a thin veneer of GE7031 varnish to a flattened, crossed thermocouple junction (made of 12.5-μm-diam Chromel and Constantan wires) which has been varnished to a Mylar frame that provides rigid support. The ends of the thermocouple wires are then attached to copper connecting pins in thermal contact with the heat sink that serve as reference junctions for the thermocouple. A light shield is placed over these pins to prevent heating by the light pulses. The front face of the sample is coated with a colloidal graphite suspension (DAG) to avoid spurious effects from changes in absorptivity at T_c. Helium gas surrounds the sample and provides the main thermal contact between the sample and heat sink. The light from an external quartz-iodide lamp passes through a mechanical light chopper and optical

TABLE I. Characteristics of $YBa_2Cu_3O_{7-\delta}$ samples.

Sample	Mass (μg)	Size (mm^3)	Twinning
YC180	80	$0.6\times1.1\times0.02$	Moderate
YC187	40	$0.5\times0.7\times0.02$	50% single domain
YC267	40	$0.7\times0.5\times0.02$	80% single domain

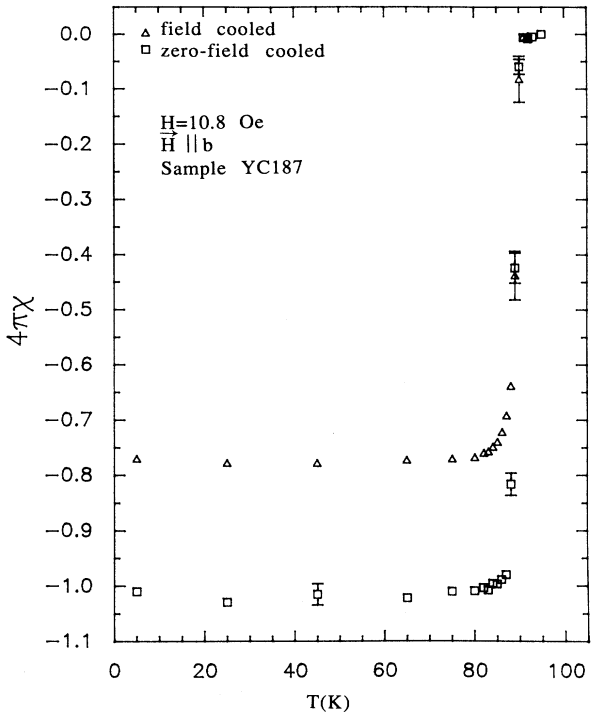

FIG. 1. Zero-field and field-cooled ($H=10.5$ Oe) diamagnetic susceptibility of sample YC267.

windows in the cryostat, resulting in a square wave heat flux

$$p(t)=\frac{1}{2}p_0\left[1+\frac{2}{\pi}e^{i\omega t}+\cdots\right]. \tag{2}$$

The modulation period $\tau_0=2\pi/\omega$ must be chosen to be long relative to the relaxation time τ_1 of the sample (in the z direction) but short compared with the sample-bath relaxation time τ_2 ($\tau_1\ll\tau_0\ll\tau_2$). Here we have

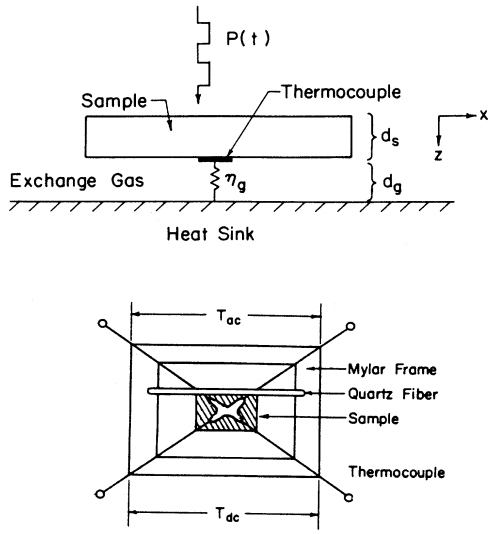

FIG. 2. Schematic of the ac calorimetry method.

$\tau_1 = C_s d_s^2/\eta_s$ and $\tau_2 = C_s d_s d_g/\eta_g$, where d_s is the sample thickness, d_g is the sample-heat sink separation, η_s and η_g are the sample and gas thermal conductivities, and C_s is the sample specific heat. Under these conditions[21] the specific heat is given by

$$C_s = \frac{p_0}{\pi\omega d_s T_{ac}} . \tag{3}$$

Because p_0 is not precisely known, the data are calibrated to match the value from a standard adiabatic heat-capacity measurement on a polycrystalline sample at 77 K; we obtain C_s (77 K) = 147 mJ/gK. The periodic heating also produces a constant temperature offset ($T_{dc} = p_0 d_g/2\eta_g$) of the sample from the heat sink, measured by the second arm of the thermocouple. A platinum temperature sensor embedded in the heat sink measures the absolute temperature; corrections for magnetoresistance were taken into account for the field measurements.[22]

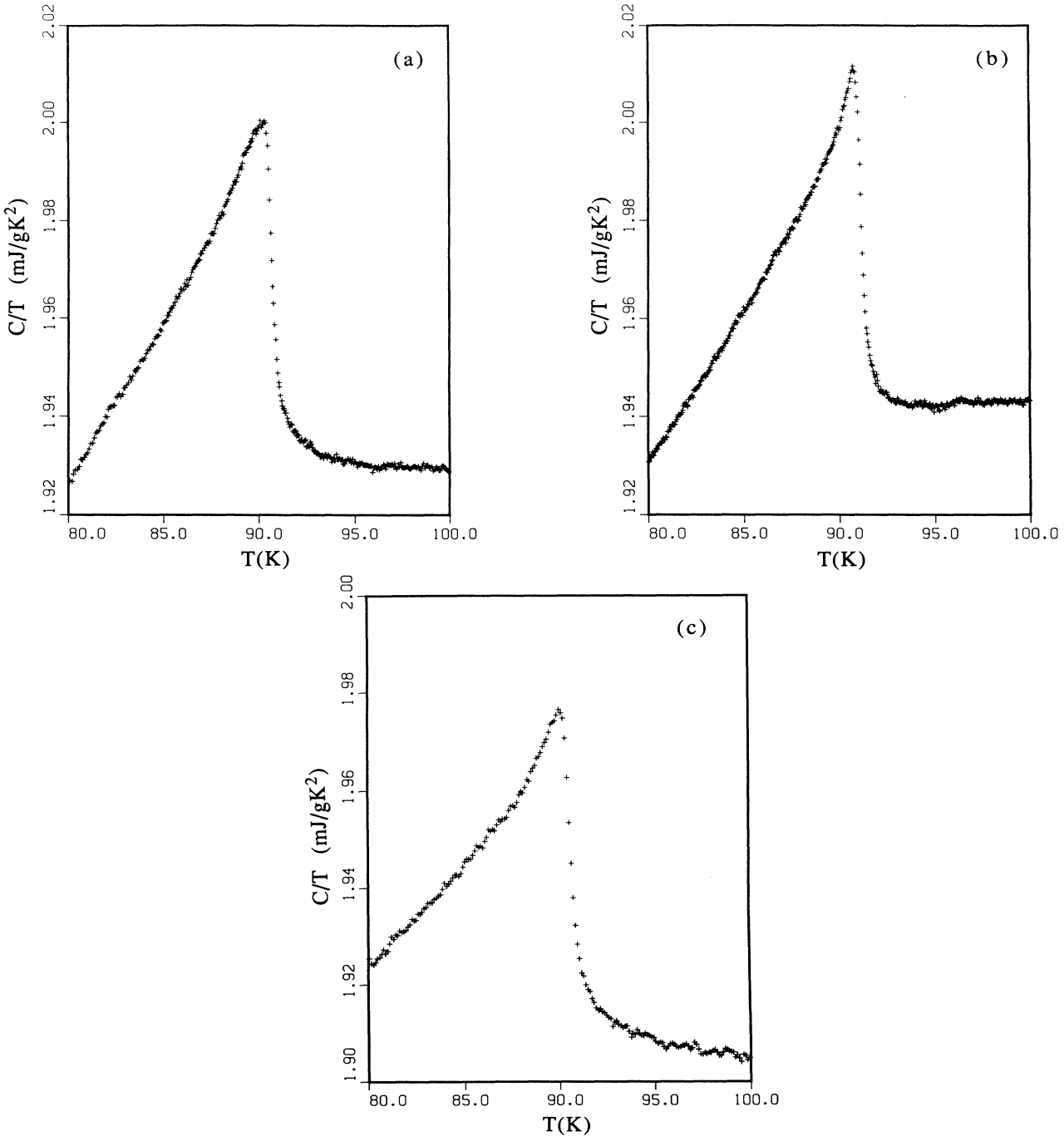

FIG. 3. C/T vs T for samples (a) YC180, (b) YC187, and (c) YC267.

For these samples ($d_s \approx 0.02$ mm), τ_1 is estimated from published values[4,23] of C_s and η_s to be on the order of 2 msec between 80 and 100 K; τ_2 was set (by controlling the He gas pressure at approximately 100 μm of Hg, with $d_g = 2$ mm) to be greater than 3 sec; τ_0 was chosen to be 167 msec (6 Hz). T_{ac} (generally less than 20 mK) was detected by a low-noise transformer and lock-in combination. The temperature sweep and data acquisition were computer controlled to a scan rate of about 0.2 K/min. No systematic difference was observed between data acquired while heating and cooling, nor for scan rates between 0.04 and 0.2 K/min. For measurements in magnetic fields, a thin quartz fiber was varnished to one side of the sample to decrease vibrations and prevent the sample from rotating in the field. Zero-field data taken before and after this fiber was attached showed no substantial difference. This can be understood as follows: if the sample were an infinite plane, the T_{ac} measured by the thermocouple would not be affected by an addition of mass to the sample far from the thermocouple. The portion of the sample that is in thermal equilibrium with the thermocouple is a cylinder of thickness d_s and a radius of a few frequency-dependent thermal lengths ($\lambda = 2\eta_s/\omega C_s < 0.25$ mm for $80 < T < 100$ K). In this case, the quartz fiber was attached at least 0.4 mm from the junction and did not appreciably affect the measured T_{ac} over the temperature range of interest.

ZERO-FIELD DATA

Zero-field data for three samples are plotted as C/T versus T in Fig. 3. Because the data for sample YC187 display the narrowest transition (< 0.5 K), we concentrate on this sample; results for the other two samples are similar but with larger uncertainties (due to the larger transition widths) and are reported in tabular form. Note that there is no strong correlation between the degree of twinning and the sharpness of the transition. There is some sample-to-sample variation in the background contribution. This variation is at least partially attributable to differing addenda contributions, but may also indicate slight variations in oxygen content between the samples.[4] Comparison of the size of the discontinuities to those of well-oxygenated samples will be made below.

We analyze the zero-field data by assuming a functional dependence for the total heat capacity and applying a Marquardt least-squares-fitting routine.[24] The contributions to the specific heat in the vicinity of T_c consist of a large phonon plus addendum background $C_{BKG}(T)$ (including the normal electronic component), an underlying mean-field step $\Delta C(T)$ for $T < T_c$, and finally the fluctuation contribution $C_{fl}(T)$. In an earlier paper,[1] we modeled $C_{BKG}(T)$ by a function linear in $t = T/T_c - 1$. To fit a wider range of data well above and below T_c and to account for the slight negative curvature of C_{BKG} near T_c, we add a quadratic term, writing $C_{BKG}(T) = a_1 + a_2 t + a_3 t^2$. Values of a_3 plotted in Fig. 4 are obtained fitting data within ± 5 K of temperatures far from T_c. Interpolation gives $a_3 = -40 \pm 20$ mJ/gK in the vicinity of T_c.

The mean-field (BCS) electronic term below T_c is given by

$$\Delta C(t) = a\gamma_0 T_c (1 + bt) , \tag{4}$$

where γ_0 is the renormalized Sommerfeld constant. The constants take on the values $a = 1.43$ and $b = 2.62$ in the weak-coupling limit, but have been observed[25] to be as large as $a = 2.6$ and $b = 4.8$ in a strong-coupling superconductor such as lead. As in our previous analysis, we allow these to vary. The leading fluctuation correction to the BCS expression arises from quadratic terms in the Ginzburg-Landau free-energy functional, the so-called Gaussian terms.[26] They are predicted[27] to have the form $C_{fl} = C_{fl}^{\pm} |t|^{-\alpha}$, where $\alpha = d\nu - 2$, d is the effective dimensionality of the superconducting electronic system, ν takes the MF value $\frac{1}{2}$, and the coefficients satisfy

$$C_{fl}^{+} = \frac{n_{eff} k_B}{16\pi\rho\xi_0^3} \tag{5}$$

and

$$C_{fl}^{-} = 2^{d/2} C_{fl}^{+} / n_{eff} . \tag{6}$$

Here ρ is the sample density (6.4 g/cm^3) and n_{eff} is the effective number of components of the Ginzburg-Landau order parameter. For anisotropic materials n_{eff} gives the dimensionality of an irreducible representation of the crystal space group, and not the order-parameter symmetry.[28] In the true critical regime, where $|T - T_c| \ll |T_g - T_c|$, fluctuations dominate the behavior.

In fitting the above contributions to the data, we fix a_3 and permit the remaining seven parameters (a_1, a_2, $a\gamma_0$, b, C_{fl}^{+}, C_{fl}^{-}, and T_c) to vary. The parameter a_3 is adjusted manually while its effect on the variance σ and on the other fitting parameters is noted. "Rounded" points within $|T - T_c| \leq 0.3$ K are not included in the fitting process. We first explore the effect of variation of α on the variance of the fit, as shown in Fig. 5, for several values of a_3. The best fit is obtained for $\alpha = 0.45 \pm 0.5$ and $a_3 = -40$ mJ/gK. When we set $\alpha = 0.5$ (three-dimensional Gaussian fluctuations), the resultant best fit is as shown in Fig. 6, with the values given in Table II.

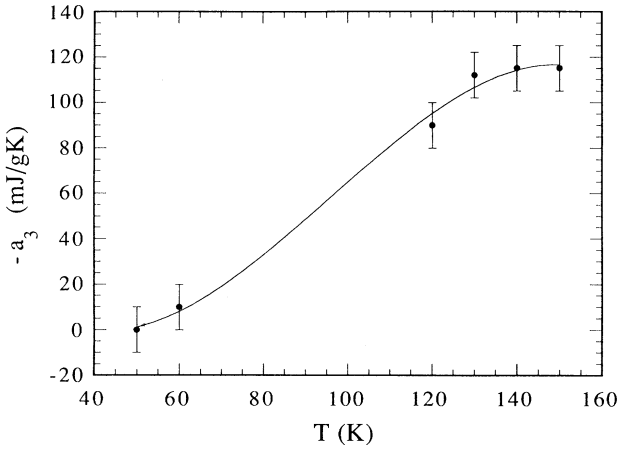

FIG. 4. Curvature a_3 of total heat capacity, determined by fitting data to a quadratic function.

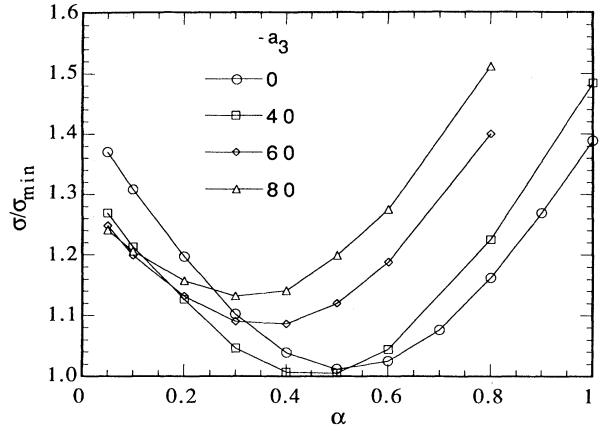

FIG. 5. Dependence of the variance of the fit on the pwoer law of the divergence α, for various estimates of the background curvature a_3. The minimum is $\sigma_m = 0.043$.

From Eqs. (5) and (6) we obtain $\xi_0 = 8.5$ Å and $n_{\text{eff}} = 2.0$. This value of n_{eff} is consistent with s-wave pairing, but does not rule out a more complicated order parameter.[28]

To estimate the uncertainty in this determination of n_{eff}, we note that the value of n_{eff} obtained is covariant with the value of T_c. Consequently, we test the effect of changing T_c on σ and n_{eff}, as shown in Fig. 7. Here the variances are scaled by the minimum variance $\sigma_{\min} = 0.043$ obtained for $T_c = 91.15$ K. Clearly, the best fit is obtained for a low value of n_{eff}; the variance with $n_{\text{eff}} = 7$ is 60% larger than that of the $n_{\text{eff}} = 2$ fit.

Because fluctuations reduce T_c from its MF value T_c^{MF}, the values obtained from the fitting analysis for $a\gamma_0$ and b are not the true mean-field values to be compared with the BCS predictions. We illustrate this in Fig. 8(a). The entropy of a superconductor with fluctuations (dashed curve) is larger near T_c than that of a reference superconductor (with no fluctuations) (solid curve) having the same T_c^{MF}. The same situation is sketched in Fig. 8(b) for the heat capacity. To determine the underlying MF behavior from the data, the total entropy of the fluctuations must be balanced by the MF entropy lost in the reduction of the critical temperature from T_c^{MF} to T_c. The total en-

TABLE II. Fitting parameters and extrapolated mean-field parameters assuming 3D Gaussian fluctuations. (Top) Fitting parameters for the lattice plus normal electronic contributions $C_{\text{BKG}} = a_1 + a_2 t + a_3 t^2$. The a_i parameters are of dimension mJ/gK. (Middle) Fitting parameters for electronic contributions. ΔC and C^+ are in mJ/gK; b and n are dimensionless. (Bottom) Mean-field electronic contribution obtained by entropy-conserving extrapolation.

Sample	a_1	a_2	$-a_3$	T_c (K)
YC180	173.9	180.1	20	90.6
YC187	175.9	189.2	40	91.15
YC267	172.4	170.0	30	90.6

Sample	$\Delta C(T_c)$	b	C_{fl}^+	n_{eff}	ξ_0 (Å)	σ
YC180	5.1	7.4	0.175	1.9	7.9	0.048
YC187	5.1	6.0	0.137	2.1	8.5	0.043
YC267	4.5	6.5	0.119	1.9	9.0	0.058

Sample	$\Delta C(T_c^{\text{MC}})$	b^{MF}	T_c^{MF}
YC180	7.2	5.2	95.6
YC187	6.6	4.6	95.9
YC267	6.7	4.6	94.9

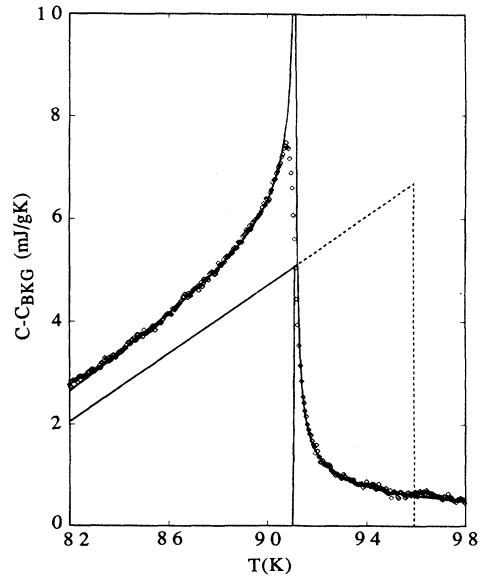

FIG. 6. Heat-capacity data (C-C_{BKG}) and fitting function for sample YC187 assuming $\alpha = \frac{1}{2}$ and $n_{\text{eff}} = 2$. The solid-line step indicates the BCS contribution. The dashed line is the result of an extrapolation of the mean-field step to account for the entropy of the fluctuations.

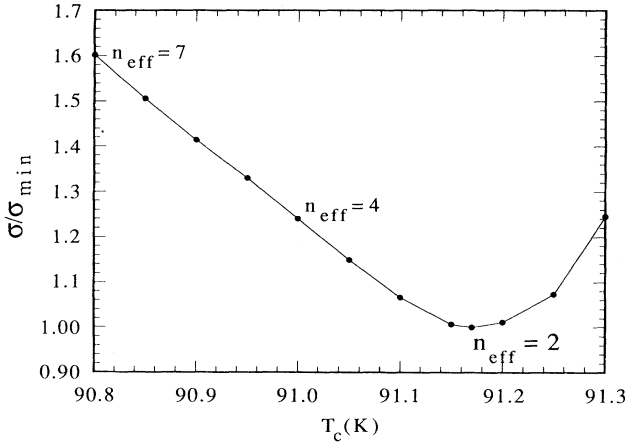

FIG. 7. Dependence of the variance of the fitting function on critical temperature for sample YC187. The best fit is obtained for $T_c = 91.15$ K, which gives $n_{\text{eff}} \approx 2$.

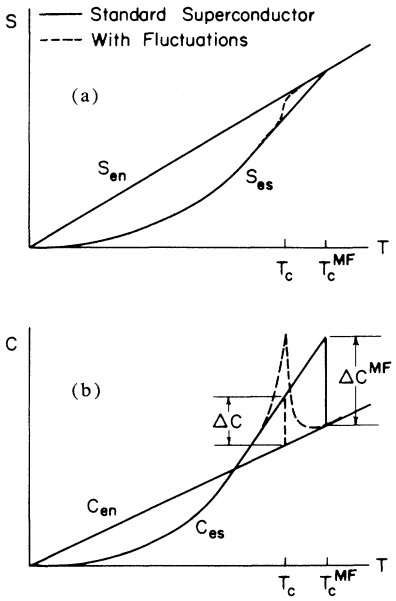

FIG. 8. (a) Electronic entropy and (b) heat capacity as a function of temperature for a standard superconductor (solid line) and for an identical system in which fluctuation effects are pronounced (dashed line). The higher entropy of the fluctuations drive the system into the normal state at a temperature T_c that is lower than the mean-field critical temperature T_c^{MF}.

tropy of the fluctuations is simply $S_{fl}=\pi(C_{fl}^{+}+C_{fl}^{-})$ for $\alpha=\frac{1}{2}$, and must equal the "missing" mean-field entropy

$$S^{MF}=\int_{T_c}^{T_c^{MF}}\frac{\Delta C(T)}{T}dT\ . \tag{7}$$

Taking into account a small (2%) correction for rounding at T_c, we obtain the extrapolation shown in Fig. 6; the values are given in Table II (bottom). The value for b is comparable to that of lead and indicates the very strong-coupling limit. Because b is sensitive to the value of a_3, we have plotted the variation of σ and b^{MF} in Fig. 9, so

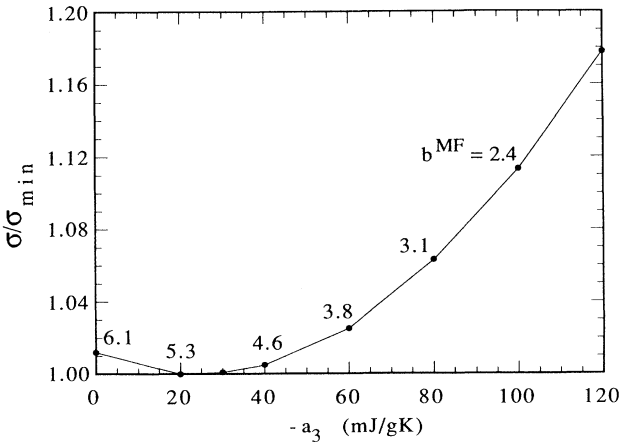

FIG. 9. Variance of the fit as a function of the estimate of the curvature a_3 of C_{BKG}. Resulting values of the mean-field slope b^{MF} are shown.

that $b=4.6\pm0.7$. The results of a similar analysis for all three samples are given in Table II. From this entropy-conserving analysis we find $\Delta C(T_c^{MF})/T_c^{MF}=46-50$ mJ/mol K^2 (48–52 mJ/mol K^2 if we assume that roughly 5% of the total heat capacity is due to addenda contributions). Other researchers have obtained values for the discontinuity by extrapolating the total heat capacity below T_c in an entropy-conserving construction. Most measurements on samples with broader transitions give $\Delta C(T_c^{MF})/T_c^{MF}$ on the order of 50 mJ/mol K.[2] However, larger values (as high as 75 mJ/mol K^2) have been reported for well-oxygenated samples with fairly sharp transitions.[4] These large values were obtained by a linear extrapolation of the C/T data from above and below T_c in an entropy-conserving fit. However, this method assumes that the change in slope about T_c of the C/T data is completely due to the change in the electronic heat capacity at T_c. Inspection of the data[4] over a larger range of T shows that this is not so: the phonon background (when plotted as C/T) peaks near 100 K and has a distinct negative curvature. Part of the change of the slope of the C/T data about T_c is due to the phonon contribution, and thus the method of linear extrapolation inherently overestimates the size of the discontinuity. Still, it is quite possible that the $\Delta C(T_c^{MF})/T_c^{MF}$ we measure is not optimal. If we assume that the optimal value is 75 mJ/mol K^2, this indicates a superconducting volume fraction of $f=0.64-0.69$ for sample YC187. This will effect our estimates of the coherence lengths and γ_0 derived from our data. The actual values of the coherence lengths are modified by a factor of $f^{1/3}$ (0.86–0.88 for sample YC187).

The value of γ_0 cannot be extracted directly from $\Delta C(T_c^{MF})$ without knowing the strong-coupling correction factor for the parameter a in Eq. (4). In general, any quantity Z^{SC} in the strong-coupling limit can be related to its weak-coupling (BCS) counterpart Z^{BCS} through a correction factor[29] $\eta_z(\omega_0)$:

$$Z^{SC}=\eta_z(\omega_0)Z^{BCS}\ , \tag{8}$$

where $\eta_z(\omega_0)$ is dependent on a single characteristic frequency ω_0 in an Einstein approximation. Akis and Carbotte[30] have considered the extreme case of a δ-function density of states for which $T_c/\omega_0=0.19\pm0.09$ gives the observed range of values for b^{MF}. Because $\Delta C(T_c)$ varies as the square of the thermodynamic critical field H_c, we take[29]

$$\eta_{\Delta C}=(\eta H_c)^2=\left\{1+\left[\frac{\pi T_c}{\omega_0}\right]\left[1.1\ln\left[\frac{\omega_0}{T_c}\right]+0.14\right]\right\}^2 \tag{9}$$

from which we obtain $\eta_{\Delta C}=2.9\pm0.7$, and

$$\gamma_0=\frac{\Delta C(T_c^{MF})}{1.43\eta_{\Delta C}T_c^{MF}}=11\pm2\ \text{mJ/mol K}^2\ , \tag{10}$$

which is similar to estimates from the magnetic susceptibility.[31] If we assume a superconducting volume fraction of $f=0.66$, we obtain $\gamma_0\approx17$ mJ/mol K^2.

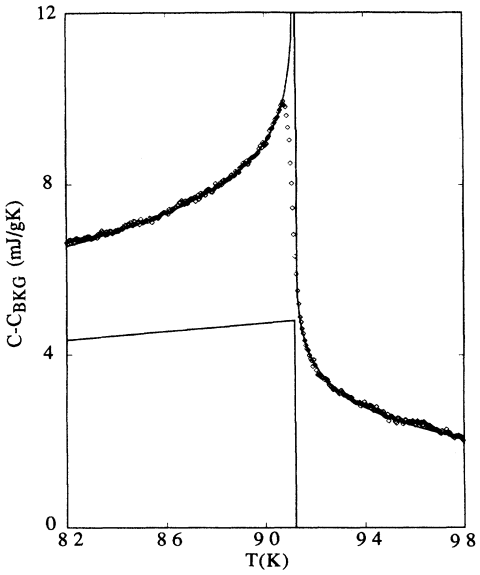

FIG. 10. Heat-capacity data (C-C_{BKG}) and fitting function for the sample YC187 assuming $\alpha=0$ ($C_{fl}\sim\ln|t|$).

We test for possible two-dimensional (2D) fluctuations by setting $\alpha=1$. The resulting fit has a 50% higher σ than the $\alpha=\frac{1}{2}$ fit. Using the fitted value $C_{fl}^{+}=0.008$ mJ/gK in Eq. (5), and assuming ξ_0^3 is replaced by $D\xi_0^2$, where D is the thickness of the superconducting sheet, we find $D\xi_0^2\approx$ (22 Å),[3] significantly larger than other estimates.[5,6,32,33]

Because the fluctuation contribution is significant we next explore the possibility of a logarithmic divergence. The result (Fig. 10) gives a variance 30% higher than the $\alpha=\frac{1}{2}$ fit. Fitting parameters for each sample are given in Table III. In each case, the best fit was obtained by using the largest value of $|a_3|$ within the acceptable range of values for that particular sample. The background heat capacity differs considerably between the logarithmic and $\alpha=\frac{1}{2}$ fits. Other researchers[5] have argued that a logarithmic singularity best describes the anomaly in $YBa_2Cu_3O_{7-\delta}$.

TABLE III. Fitting parameters assuming a logarithmic divergence. (Top) Fitting parameters for the lattice plus normal electronic contributions $C_{BKG}=a_1+a_2t+a_3t^2$. The a_i parameters are in mJ/gK units. (Bottom) Fitting parameters for electronic contributions. ΔC and C^+ are in mJ/gK; b is dimensionless.

Sample	a_1	a_2	$-a_3$	T_c (K)
YC180	172.6	192.9	40	90.7
YC187	173.6	202.1	60	91.2
YC267	170.9	179.4	50	90.7

Sample	$\Delta C(T_c)$	b	C_{fl}^{-}	C_{fl}^{+}	σ
YC180	4.6	2.0	2.4	2.0	0.053
YC187	4.8	1.0	2.2	1.8	0.055
YC267	3.9	2.2	1.7	1.4	0.059

SPECIFIC HEAT IN AN APPLIED MAGNETIC FIELD

Figure 11 shows the effect of magnetic fields up to 7 T applied both parallel and perpendicular to the c axis for sample YC267. As was observed previously[11] in polycrystalline samples, the transition is decreased in amplitude and broadened with increasing field, but with little or no shift in the onset temperature. This broadening makes a determination of $T_{c2}(H)$ rather arbitrary. We note that in the analysis of the zero-field data, the choice of $T_c(H=0)$ that minimized the variance of the fit always fell within 0.1 K of the "inflection temperature" T_i of the transition, where the negative curvature of $C(T)$ near the maximum changes to the high-temperature positive curvature. We assume this point to approximate $T_{c2}(H)$ in the field data, and determine the inflection point from the minimum of the first derivative of the data. In Ginzburg-Landau theory the upper critical field varies with temperature according to

$$H_{c2}(t)=\frac{\phi_0}{2\pi(\xi_0^{\perp})^2}|t|^{2\nu}=H_{c2}(0)|t|^{2\nu}\ , \tag{11}$$

where $\xi_0^{\perp}$ is the coherence length perpendicular to the applied field. Thus, H_{c2} varies as $|t|$ in the mean-field region and as $|t|^{4/3}$ in the critical region. Most critical field data (e.g., from resistive or magnetic transitions) show some nonlinear behavior in $H_{c2}(t)$ near T_c. The standard approach is to ignore the low-field data and to estimate $H_{c2}(0)$ from the more linear high-field data. For instance, Crabtree *et al.*[33] find from their magnetic susceptibility data ($-T_c dH_{c2}/dT$)=170 T for fields applied along the c axis, and 960 T for fields in the ab plane. For this sample the power law is approximately $\nu=0.85$ in both field directions, larger than either the expected mean-field or critical behavior. We have acquired data for several samples; in general, the power law is larger for the more heavily twinned samples, as high $\nu=1.2$ for sample YC180. Crabtree *et al.*[33] have also noted the effect of twinning on the apparent $H_{c2}(t)$, as determined from the sensitivity data, and attributed it to flux pinning. If we fit the high-field data to a linear dependence, we find $H_{c2}^{c}(0)=250\pm25$ T, $H_{c2}^{ab}(0)=1000\pm100$ T, and

$$\begin{aligned}\xi_0^{c}&=2.9\pm.4\ \text{Å}\ ,\\ \xi_0^{ab}&=11.5\pm.5\ \text{Å}\ ,\\ \xi_0&=7.5\pm.5\ \text{Å}\ .\end{aligned} \tag{12}$$

However, if we assume that $H_{c2}\propto|t|^{4/3}$, we find $H_{c2}^{c}(0)\approx600$ T, $H_{c2}^{ab}(0)\approx3000$ T, and

$$\begin{aligned}\xi_0^{c}&=1-2\ \text{Å}\ ,\\ \xi_0^{ab}&=7-8\ \text{Å}\ ,\\ \xi_0&=4-5\ \text{Å}\ .\end{aligned} \tag{13}$$

It must be understood that neither of these approaches will give the exact values of the critical fields and coher-

ence lengths, since flux pinning apparently complicates the determination of $H_{c2}(t)$ in even the best samples.

Analyses of type-II superconductors in magnetic fields have concentrated on solutions to the Ginzburg-Landau equations by perturbation methods, leading to a universal, one-dimensional scaling form for $C_{es}(H,T)/\Delta C[T_c(H)]$ where $C_{es}(H,T)$ is the superconducting electronic heat capacity below $T_c(H)$ and ΔC is the mean-field discontinuity at the observed $T_c(H)$. Thouless[12] showed that the field data could be collapsed onto a universal curve when polotted as

$$\frac{C_{es}(H,T)}{\Delta C}=g\left[\frac{T-T_c(H)}{\Delta T(H)}\right]=g(y)\ . \tag{14}$$

At its simplest, the theory[12] predicts $g(y)$ to have a 1D Ginzburg-Landau form. The field-dependent width parameter is related to the shift in T_c through

$$\Delta T(H)/T_c(0)\cong(\{C_{\rm fl}^{+}/\Delta C[T_c(H)]\}\{[T_c(0)-T_c(H)]/T_c(0)\})^{2/3}\ . \tag{15}$$

Hikama and Fujita[15] have carried out a Borel-Padé analysis and considered the effects of anisotropy to obtain improved forms of $g(y)$. The result is a broadened transition, that reaches a maximum at $y\approx -5$, and for which $g(0)\approx 0.2$. To scale our data in this fashion we subtract off the estimated background heat capacity obtained in the zero-field analysis for $\alpha=\frac{1}{2}$. In order that our data peak at $[T-T_c(H)]/\Delta T(H)=5$ and pass through $g(0)=0.2$ (Fig. 12) we must pick $\Delta C\cong C_m(H)$ and the values of $T_c(H)$ and $\Delta T(H)$ as given in the inset of Fig. 12. Clearly, the data do not scale in the superconducting regime. Further, $\Delta T(H)$ does not satisfy Eq. (15) nor does ΔC remain constant as required by the constancy of $T_c(H)$.

Because the $YBa_2Cu_3O_{7-\delta}$ in-field data do not behave as expected for a MF transition from three-dimensional to one-dimensional behavior, we consider possibility that the data satisfy scaling appropriate for the critical regime. Indeed, the effective Ginzburg criterion is relaxed in an applied field.[13] Assuming that dimensional crossover does in fact occur, we use the Ferdinand-Fisher ansatz.[18] It states that the temperature dependence of the heat capacity of a finite system can be obtained from that of an infinite system by substituting

$$t\rightarrow t^{*}=[(t+\delta_L)^2+\Delta_L^2]^{1/2}\ , \tag{16}$$

where δ_L and Δ_L describe the shift and the broadening of the transition and are dependent on the constraining length L.

At very low temperatures, the coherence length ξ_i in the direction of L may still be smaller than the length L. But at some temperature Δ_L, $\xi_i(\Delta_L)$ is on the order of L:

$$\xi_i(\Delta_L)=\xi_i^0=\Delta_L^{-\nu}\sim L\ . \tag{17}$$

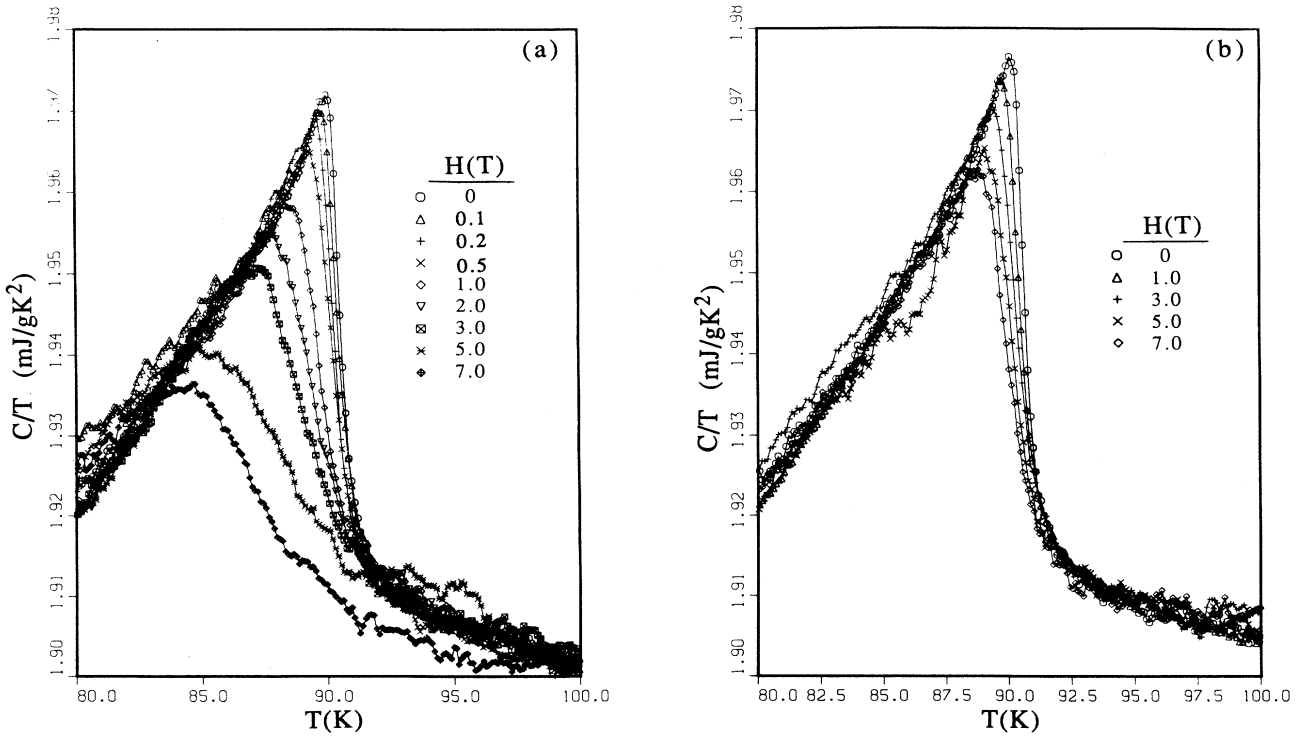

FIG. 11. $C(H,T)$ for sample YC267, with H applied (a) parallel to the c axis and (b) parallel to the ab plane.

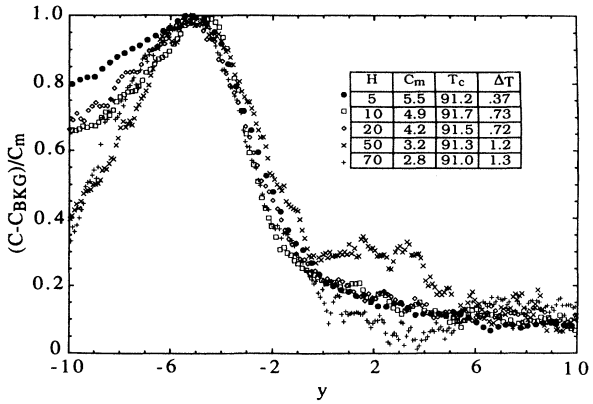

FIG. 12. Attempt to scale magnetic field data of sample YC267 according to a one-dimensional mean-field scaling function. The parameters are given in the inset.

Fisher[18] hypothesized that the finite-size parameters scale with length as

$$\delta_L \sim \Delta_L \sim (\xi_i^0/L)^{1/\nu} \tag{18}$$

for a superconductor in the field, the limiting length scale is related to the field by $L \sim H^{-1/2}$. Therefore, the width and shift parameters scale with the field as

$$\delta_L \sim \Delta_L \sim H^{1/2\nu} . \tag{19}$$

Because these parameters depend directly on H, they will hereafter be referred to a δ_H and Δ_H. Equation (16) implies that, if the zero-field fluctuation heat capacity diverges according to a power law $C_{\rm fl}^{\pm}|t|^{-\alpha}$, the heat capacity in the field will vary as

$$C_{\rm fl}(H,t) = C_{\rm fl}^{\pm}[(t+\delta_H)^2+\Delta_H^2]^{-\alpha/2} , \tag{20}$$

showing a maximum at $t=-\delta_H$, of magnitude $C_m(H)=C_{\rm fl}^{\pm}\Delta_H^{-\alpha}$.

Both Δ_H and δ_H increase with field, broadening the transition and suppressing C_m. For xy-like critical behavior, when $\nu=\frac{2}{3}$, the broadening and shift both increase as $H^{3/4}$. Neither follows Thouless' prediction of an $H^{2/3}$ and H dependence, respectively. To test this idea we define the width of the transition as $\Delta_H=[(T_i(H)-T_m(H)]/T_c(0)$, where T_m is the temperature at which the heat capacity reaches a maximum and T_i is the inflection temperature, although any comparable definition will suffice. Note that the zero-field transition is also broadened, presumably due to sample inhomogeneities. We assume that these two effects (the field broadening and the inhomogeneity broadening) are independent and therefore add in quadrature. In Fig. 13, the total width of the transition is plotted as Δ_H^2 versus $H^{3/2}$. Clearly both basal plane and c-axis data follow this law. The square root of the ratio of the slopes ($=4.4$) reflects the ratio of the anisotropic coherence lengths (ξ^{ab}/ξ^{c}). The zero-field broadening $\Delta H(0)$ corresponds to inhomogeneities on the order of $30\xi_0$. The width Δ_H and shift δ_H (defined as $[T_m(0)-T_m(H)]/T_c(0)$) are predicted to have the same H dependence in the FSS picture; we demonstrate the linear correspondence between these in Fig. 14.

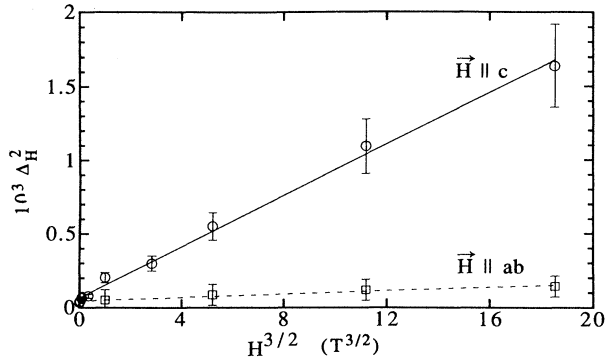

FIG. 13. Square of the total broadening of the transition $(\Delta_H)^2$ as a function of $H^{3/2}$ for sample YC267.

From Eq. (20) and for $\alpha\approx 0$, we expect the maximum of the heat capacity $C_m(H)$ to decrease in field as $\ln(\Delta_H)$. Figure 15 shows $C_m(H)$ versus $\ln(\Delta_H)$, where $C_m(H)$ has been determined by subtracting the lattice background of Table III. The FSS model correctly predicts the dependence of both the transition broadening and suppression with field, and the close correspondence between the two field directions.

Equation (20) implies that it should be possible to collapse the data by plotting them against a scaled temperature

$$y(T,H)=\frac{T-T_m(H)}{T_i(H)-T_m(H)} . \tag{21}$$

The scaling is complicated by the presence of the mean-field step underlying the fluctuation contribution and the nearly logarithmic behavior. We first subtract the normal contribution $[C_{\rm BKG}(T)]$ determined from the logarithmic fit to the zero-field data. Then, assuming logarithmic behavior, we plot the data as $C_m(H)-C_{es}(H,T)$ in Fig. 16. As predicted, the data collapse onto a single

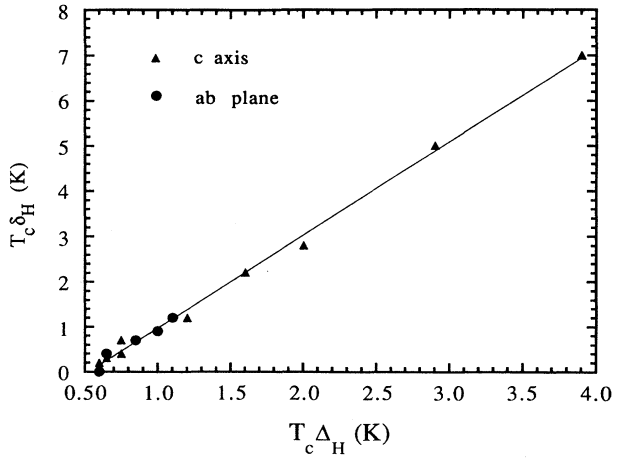

FIG. 14. Linear relation between the width Δ_H and shift δ_H of the transition, demonstrating the similar field dependence of these parameters.

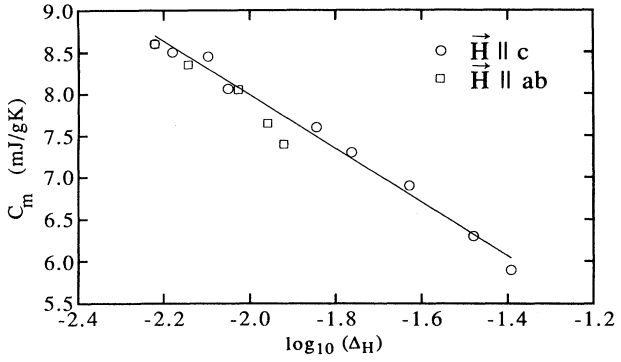

FIG. 15. Linear relation between the heat-capacity maximum $C_m(H)$ and the log of the transition width Δ_H.

curve for all fields applied both parallel and perpendicular to the c axis.

Dasgupta and Halperin[34] have performed a Monte Carlo simulation to calculate the superconducting heat capacity. We analyze our results in terms of the same FSS function used in the simulation except that we approximate the broadened step by an error function:

$$\Delta C(H)=\frac{A}{2}\left[\ln\left[\frac{(t+\delta_H)^2}{(\Delta_H)^2}+1\right]+\ln(\Delta_H)^2\right] + \frac{D}{2}\mathrm{erfc}\left[\frac{t+\delta_H}{\Delta_H}\right] . \quad (22)$$

In the absence of the broadened step, the maximum $C_m(H)$ would occur at $t_m=-\delta_H$. Because of the step, the maximum occurs at $t_m=-\delta_H-y_0\Delta_H$, where y_0 depends on the ratio D/A. We then write

$$y(H,T)=\frac{t+\delta_H}{\Delta_H}+y_0 , \quad (23)$$

$$C_m(H)=\frac{A}{2}[\ln(1+y_0^2)+\ln(\Delta_H)^2]+\frac{D}{2}\mathrm{erfc}(-y_0) , \quad (24)$$

$$C_m(H)-\Delta C(H,T)=\frac{A}{2}\ln\left[\frac{1+(y-y_0)^2}{1+y_0^2}\right] + \frac{D}{2}[\mathrm{erfc}(-y_0)-\mathrm{erfc}(y-y_0)] , \quad (25)$$

and fit the scaled data with A and D as parameters, with the result that $A=1.3$ mJ/gK, $D=4.2$ mJ/gK, (similar to the amplitude and step obtained from fitting the zero-field data to a logarithmic divergence), and $y_0=1.14$.

CONCLUSIONS

Because there is considerable ambiguity in defining the width of the critical region, we have analyzed the zero-field heat-capacity data of $YBa_2Cu_3O_{7-\delta}$ both in terms of both first-order corrections to MF theory, and of critical behavior, for three samples. Although the Gaussian fluctuation form actually gives a slightly better fit than the

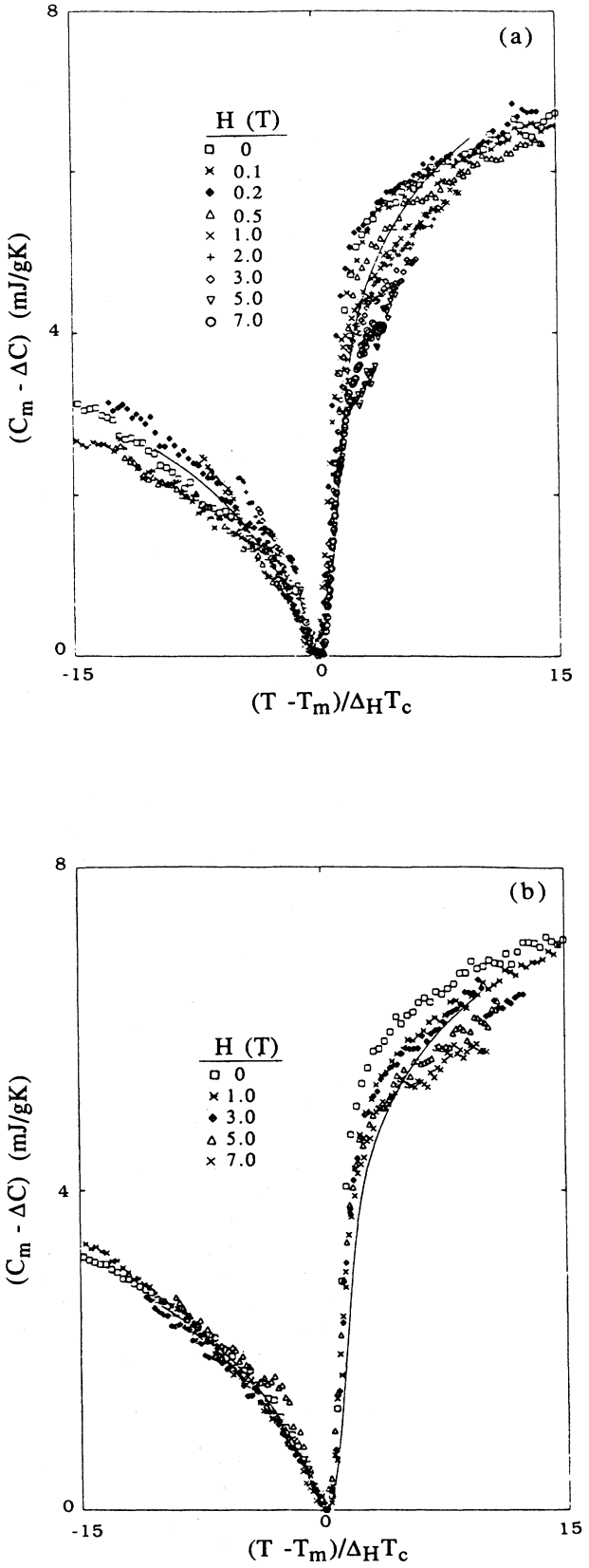

FIG. 16. Heat-capacity difference $C_m-\Delta C$ vs scaled temperature for sample YC267, (a) $H\|c$ axis and (b) $H\|ab$ plane.

logarithmic form, we cannot distinguish which is more applicable, due to the large number of fitting parameters. It is possible that the data are in a crossover regime between MF and true critical behavior. The analysis presented has concentrated on the sample with the narrowest transition; although there is some variation of the fitting parameters for the other two samples, neither shows a result that detracts the above conclusion. However, an analysis based on MF theory of the $C(H,T)$ data cannot explain either the extreme broadening of the transition or the distinct suppression of the heat-capacity peak with increasing field. Rather, both of these effects can be explained by critical finite-size effects, present because of the field-induced dimensional crossover. Indeed the data can be scaled by assuming a FSS model appropriate to a two-component order parameter in the critical regime. This result supports the general conclusion reached by Fisher, Fisher, and Huse[9] that the usual Ginzburg criterion is too restrictive. This issue will be addressed in detail in a future publication.[19]

ACKNOWLEDGMENTS

This work was supported in part by NSF Grant No. DMR-8920538 through the Illinois Materials Research Laboratory. One of us (S.I.) is supported by the Office of Naval Technology. We have benefitted greatly from discussion with Nigel Goldenfeld at every stage of this work.

[1]S. E. Inderhees, M. B. Salamon, N. Goldenfeld, J. P. Rice, B. G. Pazol, D. M. Ginsberg, J. Z. Liu, and G. W. Crabtree, Phys. Rev. Lett. **60**, 1178 (1988).

[2]S. E. Inderhees, M. B. Salamon, J. P. Rice, and D. M. Ginsberg, Phys. Rev. Lett. **66**, 232 (1991).

[3]K. Fossheim, O. M. Nes, and T. Laegrid, Int. J. Mod. Phys. B **2**, 1171 (1988).

[4]A. Junod, A. Benzige, and J. Muller, Physica C **152**, 50 (1988); N. E. Phillips *et al.*, Phys. Rev. Lett. **65**, 357 (1990); A. Junod, *Physical Properties of High Temperature Superconductors II* (World Scientific, Singapore, 1990), Chap. 2.

[5]W. Schnelle *et al.*, Physica C **168**, 465 (1990).

[6]C. J. Lobb, Phys. Rev. B **36**, 3930 (1987).

[7]M. B. Salamon, *Physical Properties of High Temperature Superconductors I* (World Scientific, Singapore, 1989).

[8]V. L. Ginzburg, Fiz. Tverd. Tela (Leningrad) **2**, 2031 (1960) [Sov. Phys. Solid State **2**, 1824 (1960)].

[9]Daniel S. Fisher, Matthew P. Fisher, and David A. Huse, Phys. Rev. B **43**, 130 (1990).

[10]L. J. Barnes and R. R. Hake, Phys. Rev. **153**, 435 (1967); S. P. Farrant and C. E. Gough, Phys. Rev. Lett. **34**, 943 (1975).

[11]R. A. Fisher, J. E. Gordon, S. Kim, N. E. Phillips, and A. M. Stacy, Physica C **153-155**, 1092 (1988); M. B. Salamon, S. E. Inderhees, J. P. Rice, B. G. Pazol, D. M. Ginzberg, and Nigel Goldenfeld, Phys. Rev. B **38**, 885 (1988).

[12]D. J. Thouless, Phys. Rev. Lett. **34**, 946 (1975); G. J. Ruggieri and D. J. Thouless, J. Phys. F **6**, 2063 (1976).

[13]Patrick Lee and Subodh R. Shenoy, Phys. Rev. Lett. **28**, 1025 (1972).

[14]Alan J. Bray, Phys. Rev. B **9**, 4752 (1974).

[15]S. Hikama and A. Fujita, Phys. Rev. B **41**, 6379 (1990).

[16]L. J. de Jongh, Solid State Commun. **70**, 955 (1989).

[17]Francis M. Gasparini, Tar-pin Chen, and Bidyut Bhattacharyya, Phys. Rev. B **23**, 5797 (1981).

[18]M. E. Fisher and A. E. Ferdinand, Phys. Rev. Lett. **19**, 169 (1967); M. E. Fisher and M. N. Barber, *ibid.* **28**, 1516 (1972); K. Binder, Ferroelectrics **73**, 43 (1987).

[19]G. Mozurkewich, M. B. Salamon, and S. E. Inderhees, Phys. Rev. B **46**, 11 914 (1992).

[20]J. P. Rice, B. G. Pazol, D. M. Ginzberg, T. J. Moran, and M. B. Weissman, J. Low Temp. Phys. **72**, 345 (1988).

[21]Ya A. Kraftmakher, *Specific Heat of Solids* (Hemisphere, New York, 1988), p. 299; P. Sullivan and G. Seidel, Phys. Rev. **173**, 697 (1968).

[22]H. H. Sample, B. L. Brandt, and L. G. Rubin, Rev. Sci. Instrum. **53**, 1129 (1982).

[23]V. Bayot *et al.*, Solid State Commun. **63**, 983 (1987).

[24]Philip R. Bevington, *Data Reduction and Error Analysis for the Physical Sciences* (Mc-Graw Hill, New York, 1969).

[25]J. E. Neighbor, J. F. Cochran, and C. A. Schriffman, Phys. Rev. **155**, 384 (1967).

[26]V. Y. Skocpol and M. Tinkham, Rep. Prog. Phys. **38**, 1049 (1975).

[27]D. J. Thouless, Ann. Phys. (N.Y.) **10**, 553 (1960); L. G. Aslamazov and A. I. Larkin, Fiz. Tverd. Tela (Leningrad) **10**, 1104 (1968) [Sov. Phys. Solid State **10**, 875 (1968)].

[28]J. Annett, M. Randeria, and S. R. Renn, Phys. Rev. B **38**, 4660 (1988).

[29]T. P. Orlando *et al.*, Phys. Rev. B **19**, 4545 (1979).

[30]R. Akis and J. P. Carbotte, Physica C **157**, 395 (1989).

[31]B. Batlogg, Physica B **169**, 7 (1991).

[32]V. Z. Kresin and S. A. Wolf, J. Superconduc. **1**, 143 (1988); T. K. Worthington, W. J. Gallagher, and T. R. Dirfer, Phys. Rev. Lett. **59**, 1160 (1987).

[33]G. W. Crabtree *et al.*, *Proceedings of the European Conference on High-T_c Thin Films and Single Crystals, Ustron, Poland* (World Scientific, Singapore, 1990).

[34]C. Dasgupta and B. I. Halperin, Phys. Rev. Lett. **47**, 1556 (1981).